Thermal quenching of bound exciton emission due to phonon-induced non-radiative transitions: experimental data for CdTe and InP

1992 J. Phys.: Condens. Matter 4 859

(http://iopscience.iop.org/0953-8984/4/3/025)

J. Phys.: Condens. Matter 4 (1992) 859–868. Printed in the UK

Thermal quenching of bound exciton emission due to phonon-induced non-radiative transitions: experimental data for CdTe and InP

H Zimmermann, R Boyn and K Piel
Fachbereich Physik der Humboldt-Universität zu Berlin, Institut für Optik und Spektroskopie, Invalidenstraße 110, 1040 Berlin,
Federal Republic of Germany

Received 28 June 1991

Abstract. The thermal quenching of (A^0X) and (D^0X) emission lines due to processes of the type $(A^0X) \rightarrow A^0 + X$ and $(D^0X) \rightarrow D^0 + X$, respectively, is discussed in terms of non-radiative phonon-induced transitions. The onset and the strength of the quenching are determined by the exciton–impurity binding energy as well as the amount of lattice relaxation accompanying these transitions. The latter effect, which has obviously been overlooked in earlier discussions, depends upon the degree of localization of the 'persistent' particle (hole or electron, respectively) and is relatively strong in the case of the 'deep' acceptors (such as Cu_{Cd} and Ag_{Cd} in CdTe). The quantitative correlation of the quenching parameters (and also of the capture coefficients related to the inverse processes) with the ionization energies of A^0 and D^0, which is expected on this basis, is confirmed by experimental results for CdTe and InP.

1. Introduction

There are many discussions of the mechanisms responsible for the thermal quenching of bound exciton emission. Starting from the first papers on this subject in the early 1970s (e.g. [1]), these discussions have been based on approximating the temperature dependence of emission intensity (I) by expressions of the type

$$I(T) \sim (1 + C \exp(-E/kT))^{-1} \tag{1a}$$

or

$$I(T) \sim (1 + C_1 \exp(-E_1/kT) + C_2 \exp(-E_2/kT))^{-1} \tag{1b}$$

and relating the energy values (E, E_1, E_2) to processes which involve the removal of certain electronic particles from the impurity centre [2].

With very few exceptions [3] the magnitudes of the pre-exponential factors (C, C_1, C_2), which should contain information on those processes, have not been analysed. Such an analysis seems particularly important when an attempt is made to answer the old question of why, in certain materials including CdTe [4–6], the (A^0X) emission lines are quenched earlier than the lines due to donor bound excitons, although the exciton binding energies are larger in the former case. This question was also not

0953-8984/92/030859 + 10 $03.50

Table 1. Parameter values for CdTe.

	Cu_{Cd}	Ag_{Cd}	P_{Te}	Li/Na_{Cd}	D
E_i (meV) [7, 8]	146	107.5	68.2	58/58.7	14
E_B (meV) [7, 8]	6.54	7.62	7.13	6.87/6.94	3.1
$\bar{C}_{fit}$ ($K^{-3/2}$)	30			20	0.04
$\bar{C}_{calc}$ ($K^{-3/2}$)	36.9	45.9	8.35	2.37	0.12
η (10^{-8} cm^3 s^{-1})	130	130	26	7.7	2.6

discussed in detail in our recent publication on CdTe [6], in which we determined the temperature dependences of bound exciton intensities using a decomposition into Lorentzian lines.

In the present paper we give a general discussion of thermal quenching for the 'classical' (A^0X) and (D^0X)-type bound excitons in terms of phonon-induced non-radiative transitions. On this basis we perform a quantitative analysis of our earlier quenching data [6] for CdTe and of new experimental results for InP.

2. Discussion of non-radiative transitions

In its general aspects, the following discussion applies to most semiconductor materials; quantitative arguments will be given for CdTe. The most probable mechanism of thermal quenching from the physical point of view is the thermal release of an exciton, i.e.

$$(A^0X) \rightarrow A^0 + X \tag{2}$$

$$(D^0X) \rightarrow D^0 + X \tag{3}$$

because the energies (E_B) involved in these processes (6–7 meV for (2) and 3.1 meV for (3), see table 1) are much smaller than the energies required for releasing single electrons or holes (or other combinations of particles).

To be specific, let us first refer to processes of type (2), which we now discuss on the basis of a configuration coordinate diagram (figure 1). The important point, which has been overlooked in earlier discussions (e.g. [2]), is that there should be appreciable lattice relaxation (shift of the minima of the configuration curves) when going from (A^0X) to $A^0 + X$ (and also from (A^0X) to A^0), because the orbital of the hole 'persistent' at the acceptor is much more strongly localized in the final state. This is immediately obvious from electrostatic considerations and from the fact that, in general, the orbital radii in the A^0 (ground) states should be considerably smaller than the effective-mass value of about 1.3 nm. The second argument applies particularly to the deeper acceptors as Cu, Ag and P, whose ionization energies (E_i) are much larger than the effective-mass value of about 57 meV (table 1).

The shift of configuration curve minima implies an increase of vibrational overlap and should thus enhance the transition rate (2). This effect should tend to decrease with decreasing E_i and should further decrease when going to the (D^0X) case (3), since the D^0 radius is rather large (close to the effective-mass value of about 5.6 nm).

The effects contributing to the variation of the transition probability can be visualized in more detail by relating the parameters of the electronic states to the phonon spectrum

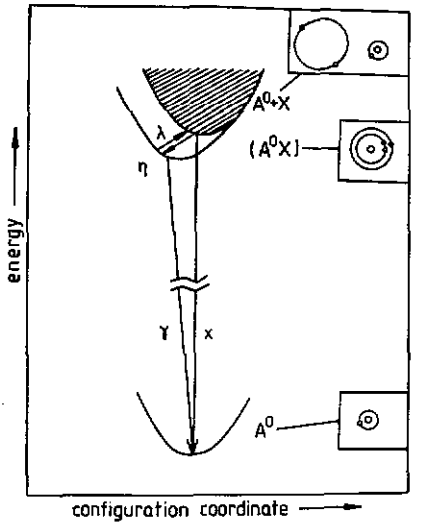

Figure 1. Configuration coordinate diagram for an acceptor centre illustrating the lattice relaxation connected with the change in the degree of localization of the orbital of the 'persistent' hole.

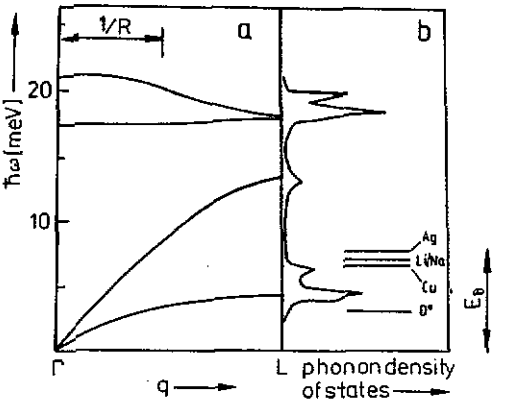

Figure 2. Phonon dispersion curves in the Γ–*L* direction (*a*) and phonon density of states (*b*) for CdTe after [9] illustrating the range of phonon states which contributes to the thermal release (and capture) of excitons (*R* orbital radius of A^0 or D^0, E_B exciton binding energy).

(figure 2) [9]. The transition probability should be dominated by contributions of phonons with $|q| \lesssim 1/R$ (q is the phonon wavevector, and R the orbital radius of the hole (electron) in the A^0 (D^0) state); so the number of phonon states making a contribution will decrease with growing R (figure 2(*a*)†). There is a second limitation with respect to the energies of the phonons involved in processes (2) and (3); these should be comparable to, or smaller than, the exciton binding energies (E_B). As a consequence, in the (A^0X) and (D^0X) case we are concerned with maximum energies above and below, respectively, the main TA peak (figure 2(*b*)).

Hence, from the viewpoint of the strength of electron–phonon interaction, process (2) is favoured compared to (3) in the twofold respect. We expect that the effects considered will manifest themselves in a tendency of decreasing pre-exponential factors in expressions such as (1), in the sequence, deeper acceptors → shallower acceptors → shallow donors, and that this can overcompensate, in many cases, the influence of the decreasing binding energies of excitons.

An analogous trend should appear for the capture coefficients for the capture of excitons by the impurities (processes inverse to (2) and (3))‡. As discussed in section 4 the trends in the two sets of data are really observed experimentally.

† A trend based on the same effect is found in the relative strengths of LO phonon satellites of the bound exciton emission lines due to radiative transitions of type $(A^0X) \rightarrow A^0$ (for CdTe see [7] figure 1). The significance of lattice relaxation effects as considered here is also evident from (integral) Huang–Rhys factors of the order of unity for acoustic phonons as estimated from the strength of corresponding sidebands in the case of CdS [10].

‡ An adequate theoretical treatment of these non-radiative transitions seems not to be available. An obvious difficulty lies in the fact that, for (A^0X), the lattice relaxation energy $\hbar\omega S$ (where $\hbar\omega$ is the characteristic phonon energy, and S the integral Huang–Rhys factor) is comparable to the transition energy E_B. This is a case to which the general treatments of non-radiative processes performed so far are not applicable [11].

3. Kinetic considerations

In our experiments on CdTe [6] and InP (section 4.2) we have studied the thermal quenching of bound-exciton photoluminescence under excitation in the interband region. In discussing such data one is faced with the problem of eliminating the temperature dependence of the concentration of free excitons, from which the bound excitons are primarily formed [12, 13] by capture processes inverse to (2) and (3). We have done this by considering ratios (V) of bound to free exciton line intensities (areas of zero-phonon lines)

$$V = I/I_x. \tag{4}$$

We think that this procedure is more reliable than analysing I-values measured under intra-impurity (dye-laser) excitation as practised, e.g. in [3] (see also [2]). This is because the results of such an analysis depend on whether the rates of the capture processes referred to above are large or small against other types of annihilation rates of free excitons (including non-radiative annihilation at other kinds of defects) [3], which should vary from sample to sample.

On the basis of figure 1 we have, for each type of (A^0X) and for (D^0X) under stationary conditions,

$$0 = \dot{n} = \eta n_x N^0 - (\gamma + \lambda)n \tag{5}$$

(N^0 is the concentration of the specific type of neutral impurity, n the part of N^0 with bound excitons, n_x the concentration of free excitons, η the capture coefficient; and γ and λ the probabilities of the radiative annihilation and thermal release of bound excitons, respectively). Strictly speaking, the first term on the right-hand side is $\sim N^0 - n$, but this may be replaced by N^0 at moderate excitation rates [14]. From (5) we get for V (see (4))

$$V = \gamma n/x n_x = \eta N^0/x(1 + \lambda/\gamma) \tag{6}$$

(x is the zero-phonon radiative annihilation probability of free excitons). Assuming that η, N^0, x, and γ are weakly temperature-dependent compared with λ we find

$$V(T) = V(0)(1 + \lambda/\gamma)^{-1} \tag{7}$$

where $\lambda\,(T = 0) = 0$ has been taken into account. The detailed balance principle yields

$$\lambda = (g'/g'')N_x(T)\eta \exp(-E_B/kT) \tag{8}$$

where g' and g'' are the degeneracy factors of the impurity state without and with the bound exciton, respectively, and

$$N_x(T) = 8(MkT/2\pi\hbar^2)^{3/2} \tag{9}$$

is the effective density of states of free excitons (M is the total effective mass of the exciton). Hence

$$V(T) = V(0)[1 + \bar{C}T^{3/2} \exp(-E_B/kT)]^{-1} \tag{10}$$

where

$$\bar{C} = 8(Mk/2\pi\hbar^2)^{3/2}(g'/g'')(\eta/\gamma) \tag{11}$$

is considered to be T-independent.

Equation (10), which is similar to the empirical equation (1(*a*)), will be the basis of our analysis performed in section 4. In this analysis we shall (i) regard $\bar{C}$ as a fitting parameter in order to demonstrate the trend predicted in section 2; and (ii) (for CdTe) give a quantitative discussion of $\bar{C}$ by relating it to independent experimental data, which enables us to eliminate the quantities η, γ, g', and g'' from (11).

To provide a basis for (ii) we now derive the required expression for $\bar{C}$. In [14] we have deduced the relation

$$V_1(1.8\,\mathrm{K}) = a(1.8\,\mathrm{K})g'(\eta/F)(3n_0m_0c)/(2\pi^2e^2\hbar x_1) \tag{12}$$

between the emission line intensity ratios

$$V_1 = I/I_{x1}$$

and the respective bound-exciton absorption line areas

$$a = \int \alpha(E)\,\mathrm{d}E$$

both taken at 1.8 K (α is the absorption coefficient, E the photon energy, n_0 the refractive index, F the oscillator strength for bound exciton generation, x_1 the probability of the one-LO-phonon assisted radiative annihilation of a free exciton, and I_{x1} the intensity of the corresponding phonon satellite).

Taking into account that γ is related to F through (e.g. [15])

$$\gamma = (F/g'')(2e^2n_0\bar{E}^2)/(3c^3m_0\hbar^2) \tag{13}$$

($\bar{E}$ is the line position) we get from (11) to (13)

$$\bar{C} = (x_1V_1(1.8\,\mathrm{K})/a(1.8\,\mathrm{K}))(2\pi Mk)^{3/2}(c^2/\pi n_0^2\bar{E}^2) \tag{14}$$

which does not contain η, γ, g', and g''.

4. Comparison with experimental results

4.1. CdTe

In figure 3 we present the temperature dependence of ratios V (see (4)) for two CdTe bulk samples based on a decomposition of emission spectra as described in [6]. The data in figure 3(*a*) have been reproduced from [6], while those in figure 3(*b*) have been obtained under the same experimental conditions as in [6]. In both cases it is clearly seen that (A^0X) is quenched earlier than (D^0X).

The acceptors responsible for (A^0X) in sample 1 are Li_{Cd} (or Na_{Cd}) and P_{Te} (which are separable only at 1.8 K [6]), while for sample 2 we are concerned with the (A^0X) doublet due to Cu_{Cd} [7, 14] (1.589 56 and 1.5907 eV at 1.8 K). For the donors, the sum of the $(D^0X)_1$ and $(D^0X)_2$ line intensities has been used in determining V in figure 3.

The experimental temperature dependences in figure 3 have been fitted by means of (10) using 'effective' E_B values which take into account that more than one bound-exciton level is involved in each case: $E_B = 6.9$ meV for (A^0X) in sample 1 (weighted average for Li, Na, and P), $E_B = 5.94$ meV for (A^0X) in sample 2 (average of the Cu doublet binding energies), and $E_B = 2.8$ meV for (D^0X) (average of $(D^0X)_1$ and $(D^0X)_2$ binding energies).

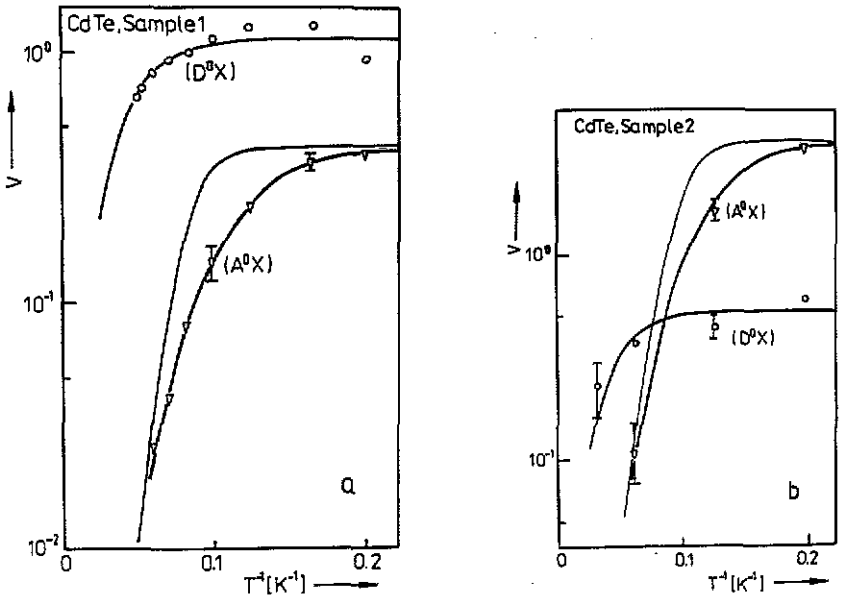

Figure 3. Temperature dependence of bound-exciton line intensities normalized to the intensity of the zero-phonon free-exciton line, for a high-resistivity n-type (*a*) and a low-resistivity p-type (*b*) CdTe bulk crystal (experimental points), and 514.5 nm Ar^+ laser excitation. The data in figure 3(*a*) have been reproduced from [6]. The dominant acceptors are Li_{Cd}, Na_{Cd}, and P_{Te} (*a*) and Cu_{Cd} (*b*). The thin curves are fits to (10); the thick curves are explained in the text.

The fits are shown by the thin solid curves in figure 3. The deviation from experiment will be discussed below. The $\bar{C}$ values obtained by this procedure are given in table 1 ('$\bar{C}_{fit}$'); they show the trend predicted in section 2.

In discussing the result in the (D^0X) case we have to consider that, different from our assumption concerning N^0 in section 3, the concentration of neutral donors is somewhat temperature dependent, due to partial recharging processes as

$$D^0 \rightarrow D^+ + e \tag{15}$$

which occur as the temperature rises [6]. This gives an additional contribution to thermal quenching. Hence, the real value of $\bar{C}_{fit}$ should be still somewhat smaller, thus enhancing the trend under discussion. $\bar{C}$ values of even smaller magnitude than for (D^0X) are estimated for (D^+X) bound excitons. For these, lattice relaxation effects as considered in section 2 are absent (as for all types of two-particle bound-excitons), and we are dealing with rather extended orbitals of the electron and the hole both before and after the quenching transition. As already mentioned, $\bar{C}$ can also be determined from independent experimental results on the basis of (14). $\bar{C}$-values deduced in this way ('$\bar{C}_{calc}$') are listed in table 1 for various impurities in CdTe, using V_1- and a-data from [14] and putting $M \approx 0.5\, m_0$, $n_0 = 3.0$, and $x_1 = 10^7\, s^{-1}$ [14]. The agreement with the $\bar{C}_{fit}$ data is quite satisfactory and the expected trend is demonstrated rather clearly, except for the inverse Cu–Ag sequence, which may be due to the effect of the impurity atoms on the phonon states. In table 1 we also reproduce η-values determined in [14]

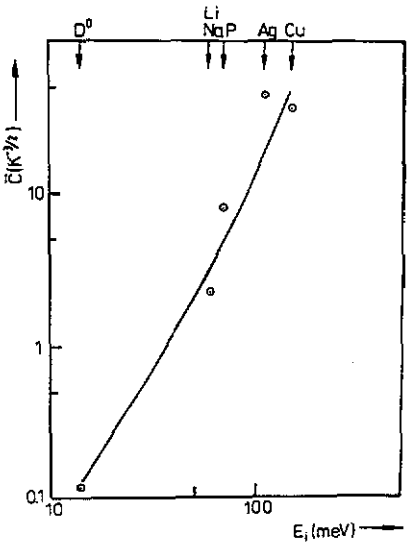

Figure 4. Correlation between the thermal quenching coefficients $\bar{C}$ (see (14)) of (D^0X) and (A^0X) and the ionization energies E_i of donors and acceptors in CdTe (see also table 1).

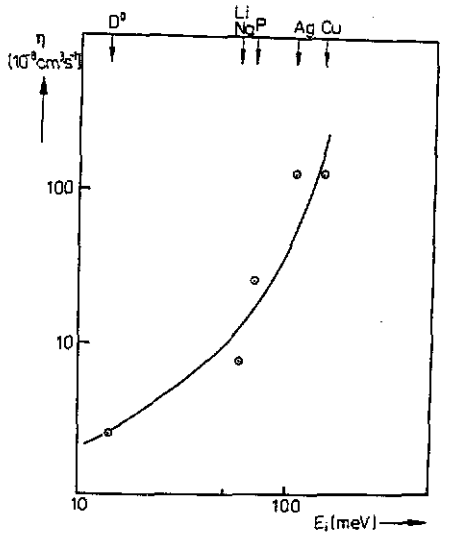

Figure 5. Correlation between the exciton capture coefficients η (determined by means of (12)) and the ionization energies E_i of donors and acceptors in CdTe (see also table 1).

with the aid of (12). Again, we observe the trend predicted earlier. The correlations of the $\bar{C}$- and η-values with E_i are also illustrated in figures 4 and 5, respectively.

Let us now discuss the systematic deviations between the fit and the experimental points for (A^0X) at intermediate temperatures. The first question to be asked is whether, contrary to our assumptions made in deriving (10), the quantities η or N^0 are temperature-dependent in the present case. From general considerations on non-radiative capture involving a single impurity level one would expect that η increases with temperature, which should lead, on the basis of (6) and (8), to a deviation in the direction opposite to the observed one. On the other hand, taking into account the large E_i-values (table 1), it seems rather unlikely that the neutral fraction of acceptors decreases by the amount necessary to explain the observed behaviour.

In principle, an explanation of those deviations can be given assuming that high-lying excited states of (A^0X) participate in the thermal release and capture of excitons, in addition to the ground state discussed so far. Because optical transitions involving such states have not been observed so far, they should have rather small oscillator strengths, which is also expected from theoretical arguments [16]. A kinetic model including such states yields, under certain conditions, an expression for $V(T)$ with an additional term $\bar{\bar{C}}\exp(-E^*/kT)$ introduced in the square brackets in (10), where E^* is the excitation energy of the bound exciton. On this basis a very good fit is possible as shown by the thick solid curves in figure 3(*a*) ($E^* = 3$ meV, $\bar{\bar{C}} = 50$) and 3(*b*) ($E^* = 3$ meV, $\bar{\bar{C}} = 70$).

4.2. InP

In figure 6 we show the excitonic emission spectrum of an epitaxial n-type InP layer at temperatures between 4.5 and 20 K. The spectrum and its temperature dependence are

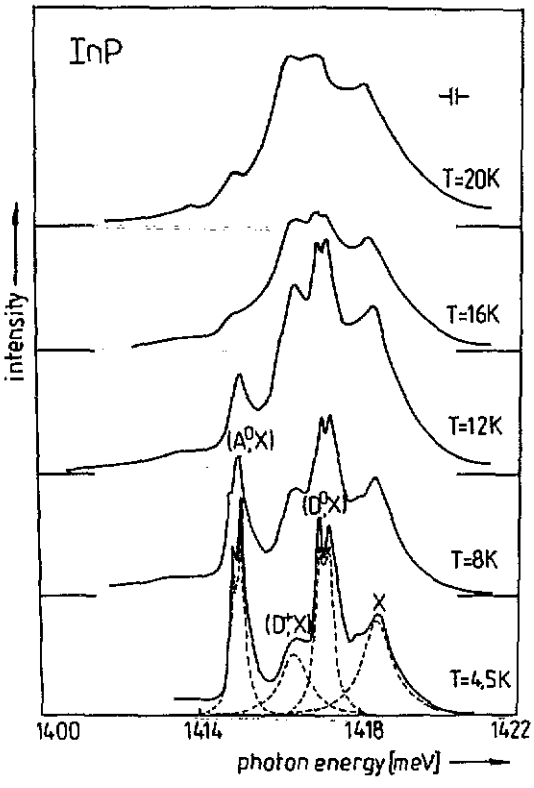

Figure 6. Temperature dependence of the emission spectrum of an n-type InP VPE layer (thickness 14 μm, InP substrate, 647.1 nm Kr^+ laser excitation). The broken curves show the decomposition into Lorentzian lines.

very similar to the CdTe case [6]; in particular, (A^0X) is quenched earlier than the donor bound excitons. As inferred from the emission spectrum in the $(D^0, A^0)/(e, A^0)$ transition range, the dominant acceptor impurity is probably C_P [17]; the nature of the donors is again unknown. The doublet structure of (A^0X) should be due to the $J = 5/2$ and $J = 3/2$ splitting components of the bound exciton ground state [18].

The spectra have been decomposed into Lorentzians by the same procedure as for CdTe [6], and the ratios V of line areas (cf (4)) are plotted as functions of temperature in figure 7 (experimental points). Here, the (A^0X) and (D^0X) values refer to sums over the (A^0X) doublet components and to sums over the $(D^0X)_1$ and $(D^0X)_2$ contributions, respectively. The fits based on (10) and the effective E_B-values $E_B = 3.5$ meV for (A^0, X) and $E_B = 1.7$ meV for (D^0, X) (compare with the values in table 2) are represented by the thin solid curves in figure 7. The resultant $\bar{C}_{fit}$ values are also presented in table 2.

The (A^0X) to (D^0X) ratio of $\bar{C}_{fit}$ is again larger than unity, but considerably smaller than the corresponding ratios for CdTe (table 1). This should be due to the following two reasons: (i) the acceptor to donor ratio of the orbital radii (R) should be larger here, as follows from the effective mass ratio (0.4 compared to 0.25 for CdTe); (ii) the energy of the TA phonon peak [19] is higher than both $E_B(A^0X)$ and $E_B(D^0X)$. As can be seen in figure 6 the (D^+X) to (D^0X) intensity ratio increases with temperature, indicating recharging processes of the type (15). Hence the real $\bar{C}$ values for (D^0X) should be somewhat smaller than $\bar{C}_{fit}$, similar to the CdTe case.

There is a deviation of the fitted curve for (A^0X) from the experimental points in figure 7, which is of the same type as (but smaller than) for CdTe and has probably the

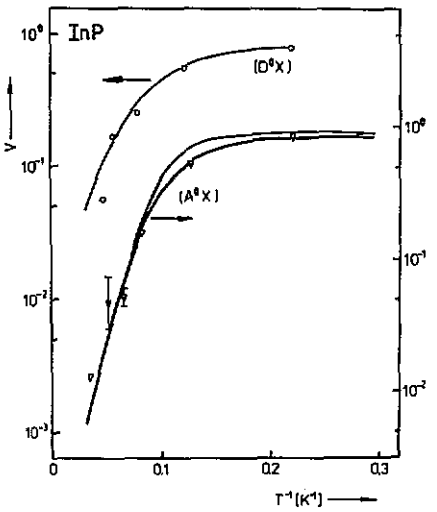

Figure 7. Temperature dependence of bound-exciton line intensities normalized to the intensity of the (zero-phonon) free-exciton line for InP (evaluated from the spectra in figure 6). The thin full curves are fits to (10); the thick curve is explained in the text.

Table 2. Parameter values for InP.

	$A(=C_p?)$	D
E_i (meV)	45	7.1
E_B (meV)	3.8	1.6
$\bar{C}_{fit}$ ($K^{-3/2}$)	2.5 ± 0.5	0.2

same reason(s) as in that case. The thick solid line in figure 7 shows a fit based on the modified form of (10) which takes into account the effect of an excited state ($\bar{\bar{C}} = 2.0 \pm 0.5$, $E^* = 1.3$ meV).

5. Conclusions

The correlation of the thermal quenching coefficients $\bar{C}$ with the impurity ionization energies E_i (as well as the analogous correlation of the capture coefficients η) which was predicted by us in section 2, has been confirmed by our experimental data. Effects of impurity-induced changes in the phonon states (related, e.g. to mass and force–constant changes), which might be expected for sufficiently strong localization of the A^0 hole, obviously only play a significant role in the Cu_{Cd}–Ag_{Cd} sequence mentioned before.

Of course, correlations of the type discussed here should also exist for other semiconductor materials. So far, data of the required kind are only available to us for Si, where capture coefficients (at 4.2 K) have been determined for various impurities. Unfortunately, there is considerable scatter between the results of different authors (typically an order of magnitude). Nevertheless, we get support for our ideas if we compare the values for shallow donors (some $10^{-8}\,cm^3\,s^{-1}$ [20–22]) with those for the deep acceptor In ($2 \times 10^{-7}\,cm^3\,s^{-1}$ [23], $2 \times 10^{-6}\,cm^3\,s^{-1}$ [24]).

Acknowledgments

The authors are indebted to Dr J Puls for valuable discussions on bound-exciton states and to Professor P Rudolph and Professor K Wandel for supplying the CdTe and InP samples.

References

[1] Bimberg D, Sondergeld M and Grobe E 1971 *Phys. Rev.* B **4** 3451
[2] Dean P J and Herbert D C 1979 *Excitons* ed K Cho (*Topics in Current Physics 14*) (Berlin: Springer) p 55
[3] Sturge M D, Cohen E and Rodgers K F 1977 *Phys. Rev.* B **15** 3169
[4] Feng Z C, Burke M G and Choyke W J 1988 *Appl. Phys. Lett.* **53** 128
[5] Giles N C, Bicknell R N and Schetzina J F 1987 *J. Vac. Sci. Technol.* A **5** 3064
[6] Zimmermann H, Boyn R, Michel C and Rudolph P 1990 *J. Cryst. Growth* **101** 691
[7] Molva E, Pautrat J L, Saminadayar K, Milchberg G and Magnea N 1984 *Phys. Rev.* B **30** 3344
[8] Pautrat J L, Francou J M, Magnea N, Molva E and Saminadayar K 1985 *J. Cryst. Growth* **72** 194
[9] Rowe J M, Nicklow R M, Price D L and Zanio K 1974 *Phys. Rev.* B **10** 671
[10] Hopfield J J 1962 *Proc. Int. Conf. Physics of Semiconductors (Exeter, 1962)* p 75
[11] Gutsche E 1982 *Phys. Status Solidi* b **109** 583
[12] Hiesinger P, Suga S, Willmann F and Dreybrodt W 1975 *Phys. Status Solidi* b **67** 641
[13] Cooper D E and Newman P R 1989 *Phys. Rev.* B **39** 7431
[14] Zimmermann H, Boyn R, Michel C and Rudolph P 1990 *Phys. Status Solidi* a **118** 225
[15] Henry C H and Nassau K 1970 *Phys. Rev.* B **4** 1628
[16] Rühle W and Klingenstein W 1978 *Phys. Rev.* B **18** 7011
[17] Skromme B J, Stillman G E, Oberstar J D and Chan S S 1984 *Appl. Phys. Lett.* **44** 319
[18] White A M, Dean P J and Day P 1974 *J. Phys. C: Solid State Phys.* **7** 1400
[19] Vandeyver M and Plumelle P 1977 *J. Phys. Chem. Solids* **38** 765
[20] Nakayama H, Nishino T and Hamakawa Y 1980 *Japan. J. Appl. Phys.* **19** 501
[21] Schramm G 1989 *Phys. Status Solidi* a **116** K209
[22] Schramm G 1990 *Phys. Status Solidi* a **120** K101
[23] Elliott K R, Smith D L and McGill T C 1977 *Solid State Commun.* **24** 461
[24] Feenstra R M and McGill T C 1980 *Solid State Commun.* **36** 1039